THE JOURNAL OF COMPARATIVE NEUROLOGY 438:318–335 (2001)

Motoneurons of Twitch and Nontwitch Extraocular Muscle Fibers in the Abducens, Trochlear, and Oculomotor Nuclei of Monkeys

JEAN A. BÜTTNER-ENNEVER,[1]* ANJA K.E. HORN,[1] HANSJOERG SCHERBERGER,[3] AND PAOLA D'ASCANIO[3]

[1]Institute of Anatomy, Ludwig-Maximilian University, Munich, Germany
[2]Division of Biology, California Institute of Technology, Pasadena, California
[3]Department of Physiology and Biochemistry, University of Pisa, Pisa, Italy

ABSTRACT

Eye muscle fibers can be divided into two categories: *nontwitch*, multiply innervated muscle fibers (MIFs), and *twitch*, singly innervated muscle fibers (SIFs). We investigated the location of motoneurons supplying SIFs and MIFs in the six extraocular muscles of monkeys. Injections of retrograde tracers into eye muscles were placed either *centrally*, within the central SIF endplate zone; in an *intermediate zone*, outside the SIF endplate zone, targeting MIF endplates along the length of muscle fiber; or *distally*, into the myotendinous junction containing palisade endings. *Central injections* labeled large motoneurons within the abducens, trochlear or oculomotor nucleus, and smaller motoneurons lying mainly around the periphery of the motor nuclei. *Intermediate injections* labeled some large motoneurons within the motor nuclei but also labeled many peripheral motoneurons. *Distal injections* labeled small and medium-large peripheral neurons strongly and almost exclusively. The peripheral neurons labeled from the lateral rectus muscle surround the medial half of the abducens nucleus: from superior oblique, they form a cap over the dorsal trochlear nucleus; from inferior oblique and superior rectus, they are scattered bilaterally around the midline, between the oculomotor nucleus; from both medial and inferior rectus, they lie mainly in the C-group, on the dorsomedial border of oculomotor nucleus. In the medial rectus distal injections, a "C-group extension" extended up to the Edinger-Westphal nucleus and labeled dendrites within the supraoculomotor area. We conclude that large motoneurons within the motor nuclei innervate *twitch* fibers, whereas smaller motoneurons around the periphery innervate *nontwitch,* MIF fibers. The peripheral subgroups also contain medium-large neurons which may be associated with the palisade endings of global MIFs. The role of MIFs in eye movements is unclear, but the concept of a final common pathway must now be reconsidered. J. Comp. Neurol. 438:318–335, 2001.

Indexing terms: extraocular motoneurons; palisade endings; myotendinous junction; eye movements; medial rectus C-group; final common pathway

Motoneurons of the extraocular muscles lie in three separate nuclei: the abducens nucleus (nVI), the trochlear nucleus (nIV), and the oculomotor nucleus (nIII). This pattern of innervation is extremely invariant throughout vertebrate evolution and probably reflects their derivation from separate rhombomeres of segmented prevertebrate ancestors (Baker, 1998). The location of the large motoneurons, characteristic of the oculomotor nuclei, has been the subject of several studies in monkey (Warwick, 1953; Augustine et al., 1981; Büttner-Ennever and Akert, 1981; Spencer and Porter, 1981). Single cell recordings, from behaving monkeys, show that all extraocular mo-

Grant Sponsor: German Research Council; Grant number: SFB 462/B3.

*Correspondence to: J.A. Büttner-Ennever, Institute of Anatomy, Ludwig-Maximilian University, Pettenkoferstr. 11, D-80336 Munich, Germany. E-mail: buettner@anat.med.uni-muenchen.de

Received 29 November 2000; Revised 29 March 2001; Accepted 20 June 2001

toneurons participate in all types of eye movements: vergence, saccades, smooth pursuit, and both vestibulo-ocular and optokinetic nystagmus (Robinson, 1970; Mays and Porter, 1984). Furthermore, the motor unit discharges are tightly linked to eye position (monkey: Keller and Robinson, 1972; Keller, 1973; man: Scott and Collins, 1973). So it is currently assumed that oculomotor commands combine at the level of the motoneurons and activate the muscle fibers through a "final common path."

The targets of this "final common path" are among the most complicated muscles of the body (review: Spencer and Porter, 1988; Porter and Baker, 1998). Eye muscles can be divided into an outer orbital layer, which consists of small caliber fibers, and an inner global layer, with larger caliber muscle fibers. There are also reports in humans of a third layer outside the orbital layer, called the marginal layer (Wasicky et al., 2000). At least six different types of muscle fibers have been identified in eye muscles, and these can be divided into two main categories: the nontwitch or multiply innervated muscle fibers (MIFs), and the twitch or singly innervated muscle fibers (SIFs) (review: Mayr et al., 1975; Morgan and Proske 1984; Spencer and Porter, 1988). The original classification by Siebeck and Krüger (1955) used the terms "Fibrillenstruktur" and "Felderstruktur" fibers, for SIFs and MIFs, respectively. The orbital and global layers of all mammals examined to date contain both fiber types. The twitch fibers, or SIFs, are the type of muscle fibers that constitute all skeletal muscles; they respond to electrical excitation with an all-or-nothing response that propagates along the whole length of the fiber. They are innervated by relatively large nerves (7–11 μm), which terminate as large *en plaque* motor endplates in an endplate zone occupying the central third of the muscle. The MIFs are highly unusual in mammals, occurring only in eye muscles, the larynx and muscles of the middle ear; but MIFs are common in amphibian muscles, and most studies have been on these preparations (review: Morgan and Proske, 1984; Dieringer and Precht, 1986). These fibers are fatigue resistant and respond to electrical stimulation with a slow tonic contraction, which is not propagated along the muscle fiber (Bondi and Chirandini, 1983). They are innervated by a myelinated nerve fiber, which usually is of fine caliber (3–5 μm). The motor endplates are typically small and are distributed all along the length of the fiber but have a higher density in the distal half of the muscle. At the distal tip of the eye muscle, as it inserts into the tendon the global layer MIFs are capped by a tangle of nerve terminals called palisade endings, or myotendinous cylinders (Dogiel, 1906; cat: Alvarado-Mallart and Pincon-Raymond, 1979; monkey: Ruskell, 1978; human: Richmond et al., 1984; Lukas et al., 2000; review, Ruskell, 1999). This characteristic is an exclusive property of the global layer MIFs, not possessed by the orbital MIFs or the SIFs.

Despite the details that are known of the anatomic organization of the eye muscle, it is not known how these structural features contribute to eye movements (Lennerstrand and Baker, 1987). The function of the palisade endings is unclear, and they are at present the subject of controversy, with some reports claiming them as sensory structures and others describing motor-like properties (Lukas et al., 2000). In addition, the role of MIF muscle fibers in eye movements is also not understood. No recordings have been knowingly made from the motoneurons supplying MIFs in awake mammals; neither is the location of motoneurons innervating MIF muscle fibers known, although they are assumed to be in the nIII, nIV, and nVI motor nuclei (Shall et al., 1995). In this study, we have attempted to locate the motoneurons of MIFs in monkeys. Small deposits of retrograde tracer were placed into distal regions of the eye muscles, avoiding the central SIF endplate zone (Fig. 1). We found that the uptake of the tracer by structures such as the fine *en grappe* endplates of the MIFs and possibly palisade endings of the global MIFs, labeled a set of peripheral subgroups around the borders of the nIII, nIV, and nVI motor nuclei, separate from the classic motoneuron subgroups. Preliminary accounts of these results have been reported at meetings (Büttner-Ennever et al., 1998; Büttner-Ennever, 2000).

Abbreviations

nIII	oculomotor nucleus
nIV	trochlear nucleus
nVI	abducens nucleus
nVII	facial nucleus
CT	cholera toxin subunit B
d	distal end
EW	Edinger-Wesphal nucleus
F	muscle fiber
G	global layer
iC	interstitial nucleus of Cajal
IO	inferior oblique muscle
IR	inferior rectus muscle
LP	levator palpebrae
LR	lateral rectus muscle
MIF	multiply innervated (nontwitch) muscle fiber
MLF	medial longitudinal fasciculus
MR	medial rectus muscle
MRF	mesencephalic reticular formation
NIII	oculomotor nerve
NIV	trochlear nerve
NVI	abducens rootlets
NVII	facial nerve
O	orbital layer
SIF	singly innervated (twitch) muscle fibers
SO	superior oblique muscle
SR	superior rectus muscle
WGA:HRP	wheat germ agglutinin horseradish peroxidase complex
WGA	wheatgerm agglutinin

MATERIALS AND METHODS

All experimental procedures conformed to the state and university regulations on Laboratory Animal Care, including the Principles of Laboratory Animal Care (NIH Publication 85-23, Revised 1985), and were approved by their Animal Care Officers and Institutional Animal Care and Use Committees.

Macaque monkeys were anesthetized with sodium pentobarbital (30 mg/kg). Under sterile conditions, the extraocular eye muscles were exposed by retracting the eyelids, making a conjunctival incision, and partially collapsing the eye ball. Large or small volumes of the neuronal tracers cholera toxin subunit B (CT, 1–10 μl, 1% from List Campbell, CA) or wheat germ agglutinin conjugated to horseradish peroxidase (WGA:HRP, 5–30 μl, 2.5% Sigma, St. Louis, MO), or iodinated WGA (^{125}I-WGA, 4–50 μl; Büttner-Ennever and Akert, 1981) were injected through a Hamilton syringe into the belly or the distal tip of the eye muscle, respectively. In several cases, two mus-

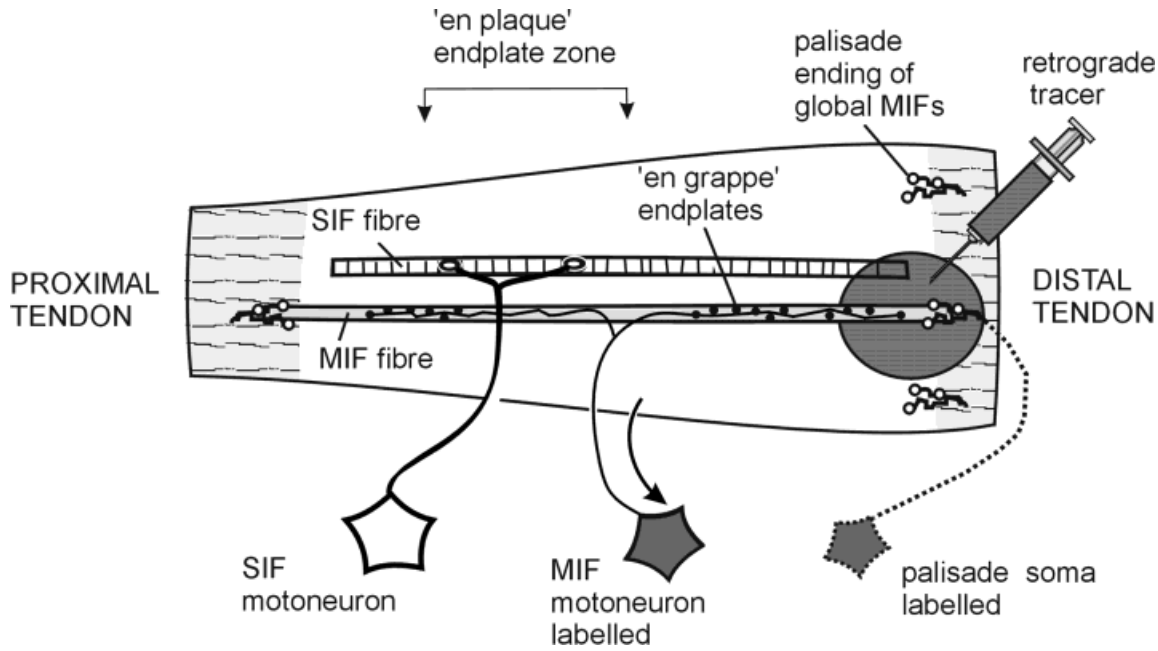

Fig. 1. Diagrammatic representation of the injections of retrograde tracer substances into the distal part of an extraocular muscle, at the myotendinous junction. The uptake area avoids the central *en plaque* endplate zone, leaving singly innervated fiber (SIF) motoneurons unlabeled. It includes *en grappe* endplates on the multiply innervated fibers (MIF), i.e., nontwitch fibers, and the palisade endings on global MIFs. The MIF motoneurons and the palisade somata will be labeled. For abbreviations, see list.

cles were injected with different tracers, and two independent series of brain sections processed for visualization.

After a survival time of 2 days (WGA:HRP), 3 days (CT), or 2–3 weeks (^{125}I-WGA), the animals were killed with an overdose of Nembutal (80 mg/kg body weight) and transcardially perfused with 0.9% saline (35°C) followed by 4% paraformaldehyde in a 0.1 M phosphate buffer solution (pH 7.4). Eye muscles were removed and stored in sucrose buffer (pH 7.4) until they were cut at 15 μm on a cryostat. The brains were immersed in 10% sucrose in 0.1 M phosphate buffer (pH7.4) and transferred to 30% sucrose for 4 days. The brain was cut at 50 or 40 μm on a freezing-microtome in the transverse plane.

To estimate the borders of the central endplate zone with respect to the injection sites, in one animal, a set of sections was taken (every 60 μm) from each of the six eye muscles; the series was mounted, and stained with anti-synaptophysin (monoclonal mouse DAKO MO776) to label endplates (Fig. 2). After suppressing endogenous peroxidase activity with 10% methanol/3% H_2O_2, and preincubation in 5% normal-horse serum + 0.3% Triton in 0.1 M phosphate buffer (pH 7.4), the sections were incubated in the anti-synaptophysin (1:20) overnight at room temperature. The incubation with the second antibody (biotinylated anti-mouse 1:200), and the visualization by using ABC kit and the diaminobenzidine (DAB) method, was similar to the methods described below for CT staining. A second set of muscle sections was stained to reveal the tracer uptake area (see below). Figure 2C shows CT-labeled palisade endings at the myotendinous junction of a medial rectus muscle fiber.

The WGA:HRP was visualized with the tetramethylbenzidine method (Mesulam, 1978). One series was usually stabilized with diaminobenzidine cobalt (Horn and Hoffmann, 1987).

For the immunocytochemical detection of CT, free floating sections of brain, or mounted muscle sections, were processed. The sections were pretreated with 10% methanol/3% H_2O_2 to suppress endogenous peroxidase activity and then preincubated in 0.1 M phosphate buffer at pH 7.4 (PB) containing 0.3% Triton X-100 with 5% normal rabbit serum for 1 hour. Then, the sections were treated with a goat choleragenoid antibody (List; 1:40,000) on a shaker for 48 hours at 4°C. Before use, the antibody was purified by a 2–12 hour absorption with chopped brain tissue of the monkey, which did not contain the tracer. The sections were washed in 0.1 M PB three times and treated with biotinylated rabbit anti-goat (1:200; Vector Labs) for 1 hour at room temperature. Then, the sections were washed in 0.1 M PB three times and incubated in avidin-biotin complex (1:50; Vector Labs) for 1 hour at room temperature. After two rinses in 0.1 M PB and one rinse in 0.05 M Tris buffer solution (TBS) (pH 8.0), the antigenic site was visualized with a reaction in 0.05% DAB and 0.01% H_2O_2 in 0.05M TBS (pH 8.0) for 5–10 minutes. The sections were mounted, air-dried, dehydrated, and cover-slipped in Depex. For orientation and analysis, alternate sets of sections were counterstained with 0.5% cresyl violet.

The ^{125}I-WGA, sections were mounted on gelatinized slides, de-fatted, rehydrated, and dried in the oven for 48 hours at 40°C. In the darkroom, the slides were dipped in Kodak NTB-3, or NTB-2, nuclear track emulsion diluted 1:1 with distilled water and dried for 4 hours. After exposure of 4 or 8 weeks at 4°C, depending on the emulsion used, the slides were developed in Kodak D-19 developer for 4 minutes at 12–15°C and fixed in Tetanal superfix (diluted 1:9 in distilled water) for 10 minutes. After wash-

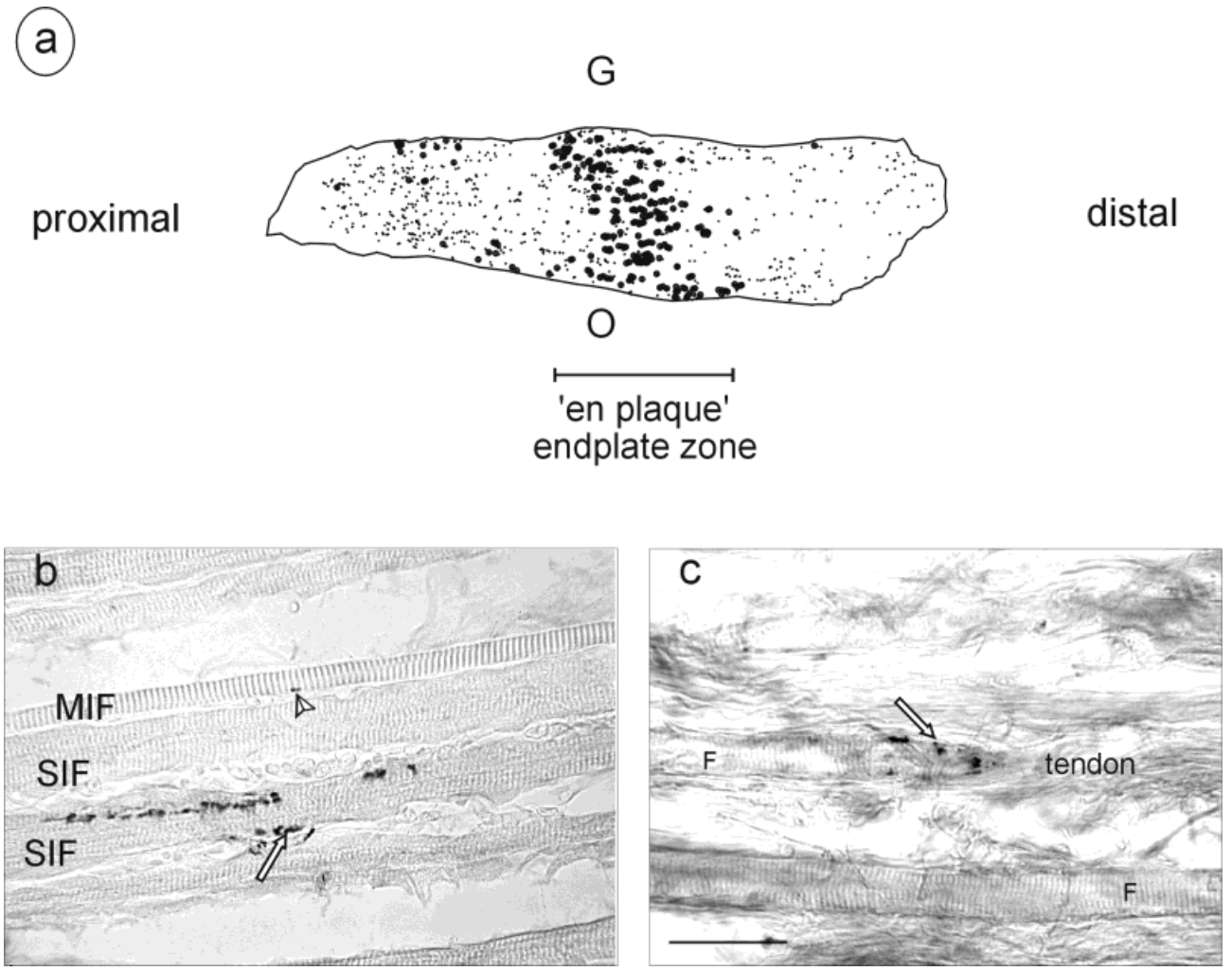

Fig. 2. **a:** The location of synaptic terminals on a 40-μm-thick section of a medial rectus (MR) muscle, labeled by synaptophysin antibody. The large dots represent *en plaque* terminals, the small dots *en grappe* or even smaller terminals. Note the central location of the *en plaque* endplate zone. **b:** A section of MR, illuminated with a lowered condenser, to emphasize the difference in the striations of the singly integrated (SIF) and multiply integrated (MIF) muscle fibers. The section is stained for synaptophysin to label *en plaque* terminals on SIFs (open arrow) and the small terminal endplates on MIFs (arrowhead). **c:** The synaptic terminals of palisade endings (arrow) labeled after an injection of cholera toxin into the adjacent tendon area. For abbreviations, see list. Scale bars = 20 μm in c (applies to b,c).

ing for 2 hours in running water, the sections were counterstained with cresyl violet, dehydrated, and coverslipped with Depex. The sections were examined and photographed by using a light microscope under darkfield and brightfield illumination.

All injection sites are treated as left eye muscle injections to facilitate the analysis. Images of brightfield photographs were digitalized by using a 3-CCD videocamera mounted on a microscope. The images were captured with 4.0 Adobe Photoshop software. After conversion into black and white, the sharpness, contrast, and brightness were adjusted to reflect the appearance of the labeling seen through the microscope.

Data analysis of cell sizes

Initially measurements of cell area/cell diameter were compiled by using a microscope and graphics board, connected to a PDP 11/12. Only labeled neurons in which the nucleus was visible were selected. The population was bimodal, and the exact location of each cell in the "small motoneuron cluster" was plotted by using black dots, whereas the location of the cells within the "large motoneuron cluster" were indicated by open circles (see Figs 7, 9, 10, and 11). In later experiments (see histograms in Fig. 13), the mean diameters (maximum diameter + minimum diameter)/2 of labeled neurons were estimated by using an image analysis system (Optimas), from images captured with a 3-CCD videocamera mounted on a microscope.

RESULTS

Abducens nucleus

Large injections into the center, or belly, of the lateral rectus (expts: 81-25, ^{125}I-WGA; H154, CT) retrogradely

labeled cells filling the whole of abducens nucleus (nVI) and surrounding the NVI rootlets (Figs. 3a,c, 4a). Some small cells were noticed around the periphery, as far medial as MLF (see arrow in Fig. 3c). An intermediate injection that mainly avoided the main endplate zone of lateral rectus (expt 81-26, ^{125}I-WGA), labeled some central abducens motoneurons but also many neurons around the borders of the nucleus (Fig. 4b). Small distal injections into the myotendinous junction of the lateral rectus near its insertion on the globe (expts. ZL1, WGA:HRP; ZL2, CT) labeled both medium-large and small cells very strongly. They lay like a shell around the medial borders of nVI, and strikingly few cells were labeled within the central core of the nucleus (Figs. 3b,d, 4c). Many small cells with a fusiform appearance were labeled; they lay amongst the rootlets of the abducens nerve as they emerged from the nucleus, or were embedded in the MLF, or were located around the facial genu. (Fig. 3c,d, 4c). These neurons lay medial to the motoneurons of the accessory lateral rectus muscle, which were not labeled in this study (Schnyder, 1984). Axons of some of the peripheral labeled cells could be followed into the abducens nerve, and in several cases, thin axon collaterals were observed.

Trochlear nucleus

Large injections into the superior oblique (SO) muscle centered on the *en plaque* endplate zone (82-572 ^{125}I-WGA) filled neurons throughout contralateral nIV (Fig. 5a). An injection into the distal SO in the region passing through the trochlea (A83-5, WGA:HRP), led to retrograde filling of a tight cluster of neurons forming a cap over the dorsal surface of the trochlear nucleus (nIV), contralaterally. Absolutely no neurons were labeled in the center of the nucleus (Figs. 5b, 6). The neurons labeled by the distal injection were slightly smaller than those in the central region of nIV (see below). Inspection of the central SO muscle sections showed that several MIFs, as judged by their characteristically conspicuous striations (e.g., compare MIF and SIF striations in Fig. 2b), had taken up the tracer from the injection site intracellularly and were filled along their length. This finding confirms the observation of Mayr et al. (1975), that some MIFs extend throughout the length of the eye muscle, in this case, extending into the injection site at the trochlea.

Oculomotor nucleus

Medial rectus muscle. Injections into the belly of the medial rectus muscle (MR) led to the labeling of several motoneuron subgroups (Expt 79-46, ^{125}I-WGA; A14-87 WGA:HRP): the A-group lying ventrally in the rostral three-quarters of the nucleus, the dorsal B-group in the caudal half, and the C-group lying just outside the classic nucleus on its dorsomedial border, and extending throughout the rostrocaudal length of oculomotor nucleus (nIII) (Fig. 7; Büttner-Ennever and Akert, 1981).

The inset graph in Figure 7 shows that the diameter profile of the MR motoneurons after a central muscle injection is bimodal. All the neurons, whose diameters fell within the first black cluster of the histogram, i.e., the small motoneurons, are shown on the neighbouring plots of the oculomotor nucleus, in Figure 7, as *filled circles*. Those motoneurons in the second white cluster, or large motoneurons, are drawn with *open circles*. The results show that smaller neurons are, in general, not scattered between the large neurons (Figs. 7 filled circles, 8a filled circles). They tend to lie separately; around the periphery of the nIII, in the C-group, around ventral border of nIII, adjacent to MLF and NIII rootlets, and some at the lateral border. A similar display of the location of large and small motoneurons in nIII labeled by central muscle injections is used in the subsequent figures (Fig. 9 for IR, Fig.10 for IO, and Fig. 11 for SR). The differences between large motoneurons within the motor nuclei and small motoneurons around the periphery are clearly visible on inspection of individual sections, under light microscopy (Fig. 8a,b, compare neurons in B and C). The mean diameter of the MR A-group and B-group motoneurons are 22.0 μm (SD = 2.7; n = 170) compared with 18.1 μm (SD = 2.6; n = 27) for the C-group (Büttner-Ennever and Akert, 1981; McClung et al., 2001). An injection into the intermediate portion of MR, avoiding the central endplate zone (Expt. H45, ^{125}I-WGA), filled fewer cells in the A and B subgroups than the central injection but a comparatively large number of C-group neurons (Fig. 7b).

Placing the tracer at the myotendinous junction, and affecting comparatively little muscle (Expt. ZL2, CT; P2, CT), led to an intense filling of neurons almost exclusively in the C-group (Figs. 7c, 8c–f), with a few strongly labeled neurons at the ventrolateral border of nIII. The remaining motoneurons in the A- and B-groups were very weakly labeled, if at all (Fig. 8c). The labeled C-group contained many medium-large neurons, and they extended more rostrally and dorsally than ever seen from the MR central or even intermediate injections (Fig. 7a,b). Neurons within this "newly labeled" portion of C-group extension encircled the lateral border of the Edinger-Westphal nucleus (EW, see Fig. 8e,f), and their extensive dendrites ramified throughout EW and the adjacent supraoculomotor area. The asterisk in Figure 8e indicates one region of intense ramifications seen in expt LZ1.

Inferior rectus muscle. A similar result was obtained with the injections of inferior rectus muscle. A central injection into the belly of the muscle (H58, ^{125}I-WGA) labeled the classic dorsal subgroup of motoneurons within nIII as well as smaller inferior rectus muscle (IR) motoneurons of the C-group (^{IR}C-group, Fig. 9). The graph of the motoneuron diameters is like that of the MR, bimodal, with the smaller cells concentrated within the ^{IR}C-group. When the tracer deposit was confined to the distal portion of the muscle, after an injection into the myotendinous junction (B55,CT.), the ^{IR}C-group was labeled exceptionally strongly (Fig. 12a,b); but very few large cells in the classic IR subgroup were filled. The presence of one or two labeled cells on the midline (marked by an arrow Fig. 12a.) was attributed to leakage of the tracer into the inferior oblique (IO) muscle (see below). The dendrites of the ^{IR}C-group neurons radiated over a large area, spreading rostrally up to the borders of EW nucleus. They did not, however, extend into EW, or spread as far laterally, as the ^{MR}C-group dendrites.

Inferior oblique muscle. Large injections into inferior oblique muscle (IO) (expts H62, ^{125}I-WGA; P2, WGA:HRP; A4-87, WGA:HRP) filled a central subgroup of motoneurons in ipsilateral nIII, as well as cells on the midline between the oculomotor nuclei, and a few cells scattered bilaterally in the neuropile around the oculomotor nucleus (Fig. 10). The small motoneurons were mainly confined to the region midway between the oculomotor nuclei, dispersed on either side of the midline, although several lay scattered around the dorsal and lateral nIII

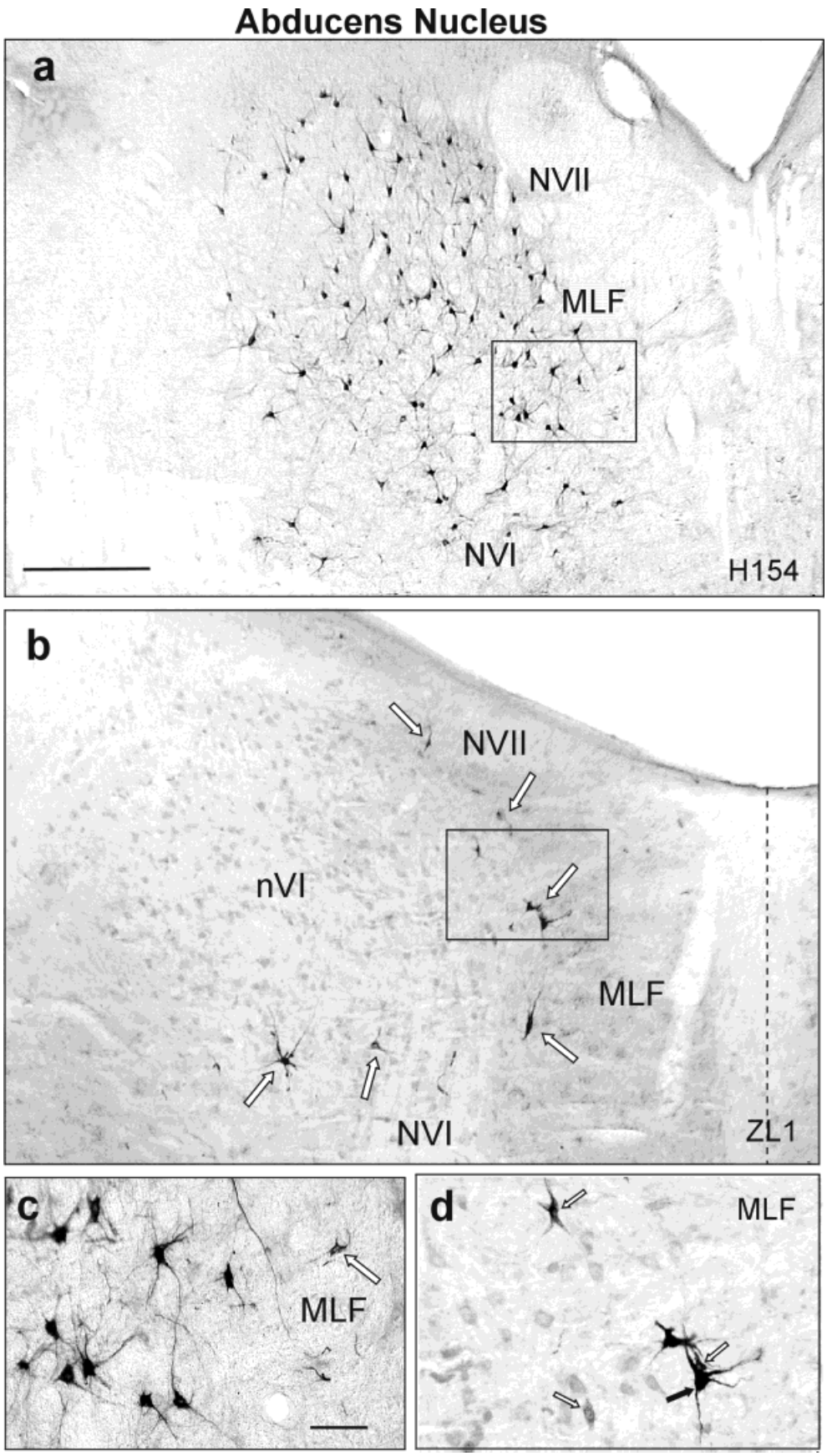

Fig. 3. **a:** Neurons in the abducens nucleus retrogradely labeled after a multiple injection of cholera toxin into the central endplate zone of lateral rectus. **b:** Retrogradely filled neurons (open arrows) labeled after a distal injection of wheat germ agglutinin horseradish peroxidase complex (WGA:HRP) into the myotendinous junction of lateral rectus, avoiding most motor endplates. Note, medium-large and small labeled cells lie around the medial borders of nVI and not in the central region. **c:** An enlargement of the square in a reveals a small caliber motoneuron in the MLF. **d:** An enlargement of the peripheral abducens neurons from the square in b, to show a large labeled neuron (black arrow) and three small labeled neurons (white arrows). For abbreviations, see list. Scale bar = 500 μm in a (applies to a,b), 50 μm in c (applies to c,d).

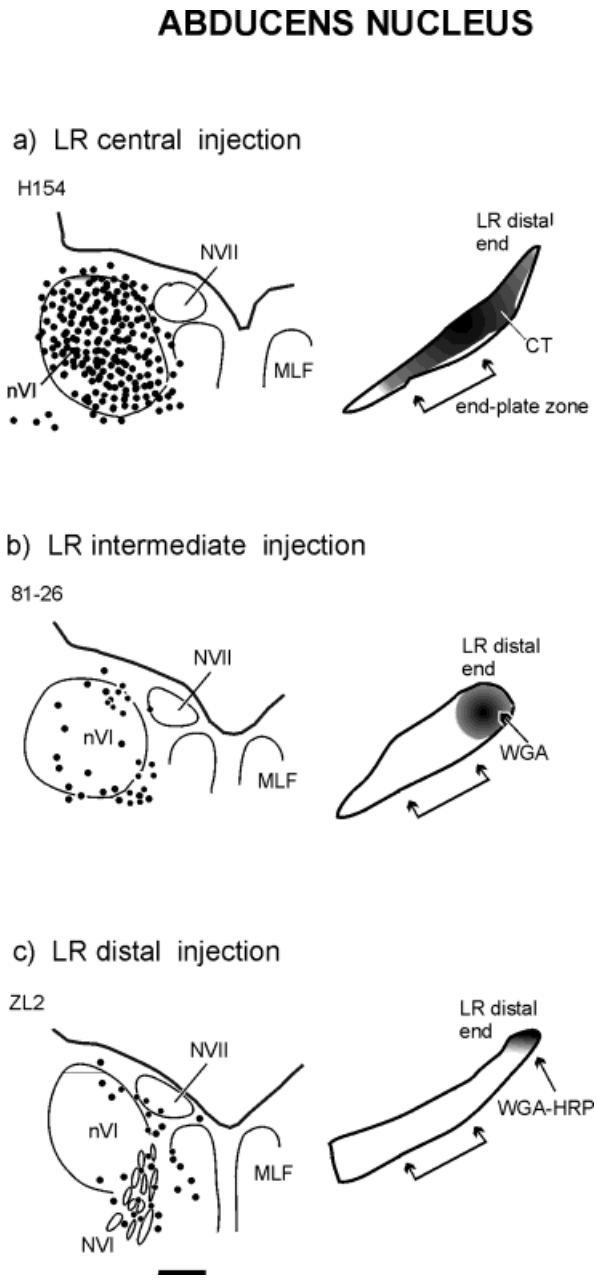

Fig. 4. **a:** A multiple central injection of CT filling the lateral rectus (LR) muscle. Note the retrogradely labeling motoneurons within the ipsilateral abducens nucleus and around the periphery (same case as Fig. 3a). The drawing is plotted from four consecutive 40-μm sections. **b:** A ^{125}I-wheat germ agglutinin (WGA) injection into the intermediate part LR retrogradely labels less central motoneurons than shown in a but several around the periphery of nVI (medial half). **c:** A WGA: horseradish peroxidase complex (WGA:HRP) injection centered on the LR distal myotendinous junction labels no central motoneurons but many neurons around the periphery of nVI and scattered in MLF. In b and c, labeled cells from six sections (40 μm) are depicted on one drawing. In both cases, the tracer spread within LR (shaded area) avoids the *en plaque* endplate zone estimated from synaptophysin-stained sections from a standard case. For abbreviations, see list. Scale bar = 500 μm.

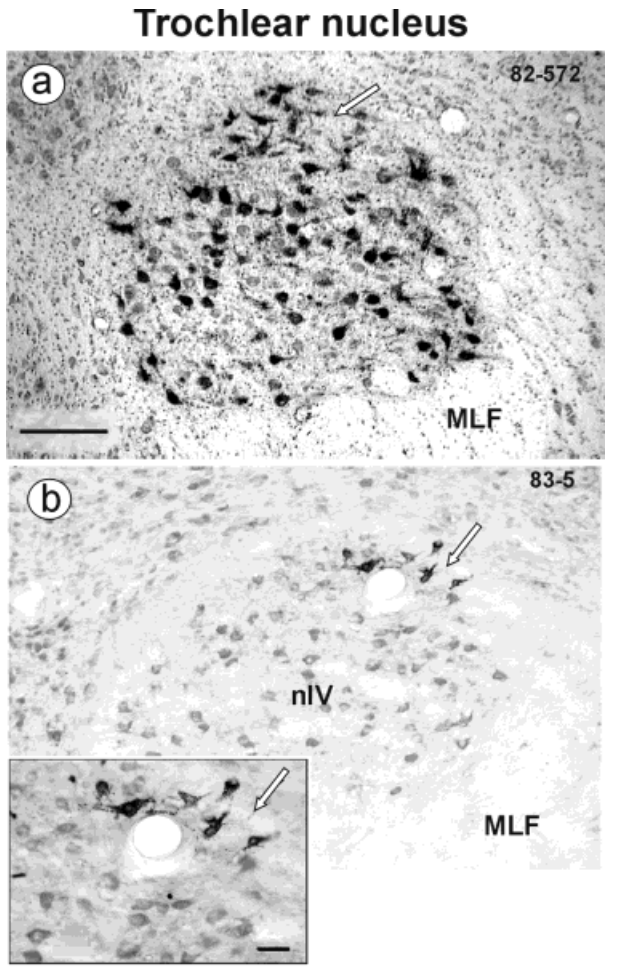

Fig. 5. **a:** An injection of radioactive wheat germ agglutinin (WGA) into the central endplate zone of SO retrogradely labels motoneurons throughout the contralateral trochlear nucleus. The arrow indicates a slightly separate cluster of neurons in the dorsal cap. **b:** An injection of WGA:HRP into the distal tip of SO, avoiding the central endplate zone, retrogradely filled a compact group of medium neurons (arrow) in the dorsal cap of nIV and none in the central region. The inset is an enlargement of the labeled cells in b. Scale bars =250 μm in a (applies to a,b), 50 μm in inset.

borders (Büttner-Ennever et al., 1982). A comparison of the large and small motoneuron diameters is provided by Figure 13a. A very distally placed injection into the myotendinous region of IO, avoiding the central endplate zone (S54 CT), labeled the midline group almost exclusively (Fig. 10). These midline neurons were scattered bilaterally but did not have such extensive dendrites as those of the $^{MR\ and\ IR}$C-group (compare Fig. 12d with 12b and Fig. 8d).

Superior rectus muscle. Finally the large injections of WGA:HRP into the mid-region of superior rectus (SR) (80-217, WGA:HRP; B26-88, WGA:HRP) labeled large motoneurons on both sides of nIII but mainly contralaterally (Fig. 11). Their distribution, by using the newer highly sensitive visualization methods, was more extensive than previously reported (Warwick, 1953). The location of the contralateral SR motoneuron subgroup coincides with that of the IO motoneurons innervating the other eye.

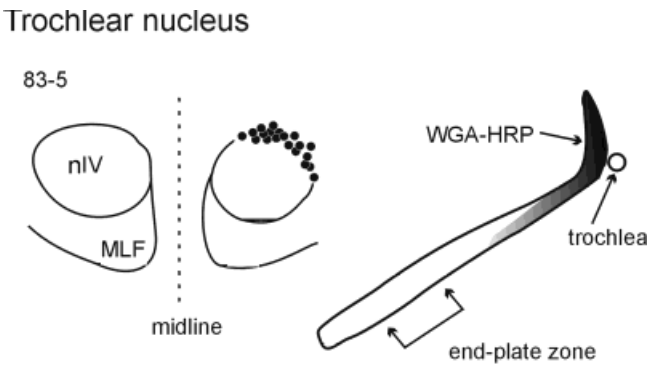

Fig. 6. Trochlear nucleus: dots represent the compact group of retrogradely labeled neurons after an injection into the distal tip of superior oblique muscle (SO). Labeled neurons from five sections (50 μm) are indicated. The tracer uptake area (shaded area) is centered on the tendon region passing through the trochlea and avoids the central endplate zone estimated from synaptophysin-stained sections from a standard case. For abbreviations, see list.

Many smaller motoneurons lay on the midline between the nIII. A small injection into distal SR (ZU,CT; B55, WGA:HRP) strongly filled midline neurons, and almost no cells within the central core of the classic nIII nucleus (Figs. 11, 12e,f). The distribution of the midline cells was bilateral and similar to IO. Like IO cells, the SR cells had sparse dendritic trees.

Data analysis of cell diameters

Figures 7, 9, 10, and 11 show that with central injections the smaller motoneurons lie around the periphery of the oculomotor nucleus. This arrangement is less clear for the abducens and trochlear nuclei. A comparison of the size of MR and IO internal motoneurons within the motor nuclei to those around the periphery of nIII (in the same experiment) is shown in Figure 13a. The neurons in the peripheral subgroups are clearly smaller, on average, than the "internal" motoneurons.

The histograms of Figure 13b compare the motoneuron populations of each muscle filled by *central injections* (grey bars), with those filled by *distal injections* (black bars). Mean diameters, etc., are given in Tables 1 and 2. There is very little difference between the histograms, with the exception of SO, where the comparison is most accurate (within the same experiment). It is extremely difficult to compare cell sizes reliably across experiments, because so many experimental factors affect cell size. However, one interesting fact emerges from this comparison, that is, the distal injections fill *both small and medium-large cells* within peripheral subgroups. This finding is different from central muscle injections where the peripheral subgroups consisted of mainly small cells (Fig. 13a). The result suggests that a new medium-large cell population is labeled from the myotendinous junction which is not labeled from the muscle belly. The difference in size between cells of the peripheral subgroups labeled from central injections (Fig. 8b, C-group) and distal injections (Fig. 8d) is evident from the photographs.

DISCUSSION

Our results show that retrograde tracer injections into the central endplate zones of the eye muscles labels large and small motoneurons and that these two populations tend to remain separate from each other. The large motoneurons lie within the classic boundaries of the extraocular motor-nuclei, whereas the smaller motoneurons cluster around the periphery (Büttner-Ennever et al., 1982). More importantly, in this study, we showed that injections into more distal parts of the eye muscle label the peripheral subgroups more strongly and more exclusively. Whether these peripheral subgroups just innervate the MIF motor endplates of the global and orbital layers or whether they are also associated with the palisade endings of global MIFs, will be critically discussed.

Do peripheral motoneurons innervate only MIFs?

Injections into the central endplate zone of the muscle, which avoid the myotendinous junction and palisade endings, clearly label many smaller motoneurons of the peripheral subgroups around the motor nuclei, like the C-group. This finding indicates that at least some cells in the peripheral subgroups supply motor endplates, and probably it is the centrally lying *en grappe* endings of the MIFs. The closer the injections to the myotendinous junction and the palisade endings, the more strongly the peripheral cell groups were labeled. The simplest explanation is to assume that this labeling is due to the additional labeling of a cell population associated with the palisade endings, and that the 'palisade' somata lie together with the peripheral motoneurons around the periphery of the motor nuclei. This explanation is tentatively supported by the analysis of the cell diameter histograms, which indicate that injections into the myotendinous junctions label a medium-large cell population which is not seen with central muscle injections (compare Fig. 13a with b). However, some caution must be taken here. Palisade endings have been shown to have branches, which extend down the MIF and terminate as endplates on MIFs (Richmond et al., 1984; Lukas et al., 2000). Because the nerve branches supplying the palisade endings, and possibly MIF endplates, run back into the tendon before leaving the muscle (Ruskell, 1978, 1999; Richmond et al., 1984; Lukas et al., 2000), damage to this nerve by the injection-pipette, and direct tracer uptake, is likely to be the reason for our intense labeling of peripheral cells by injections at the myotendinous junction and not because of the exclusive uptake by the palisade endings.

This present "muscle injection" study cannot possibly distinguish between uptake by distal endplates or palisade endings, further independent studies must be designed to decide whether the peripheral cell groups innervate the MIF motor-endplates and palisade endings. However, because both of these structures are exclusively associated with MIFs (Ruskell, 1978, 1999; Alvarado-Mallart and Pincon-Raymond, 1979; Richmond et al., 1984; Lukas et al., 2000), we can state with some certainty that our strongly labeled peripheral neurons innervate MIFs.

In addition to the intense filling of the peripheral neurons, the distal injections into any of the muscles (except

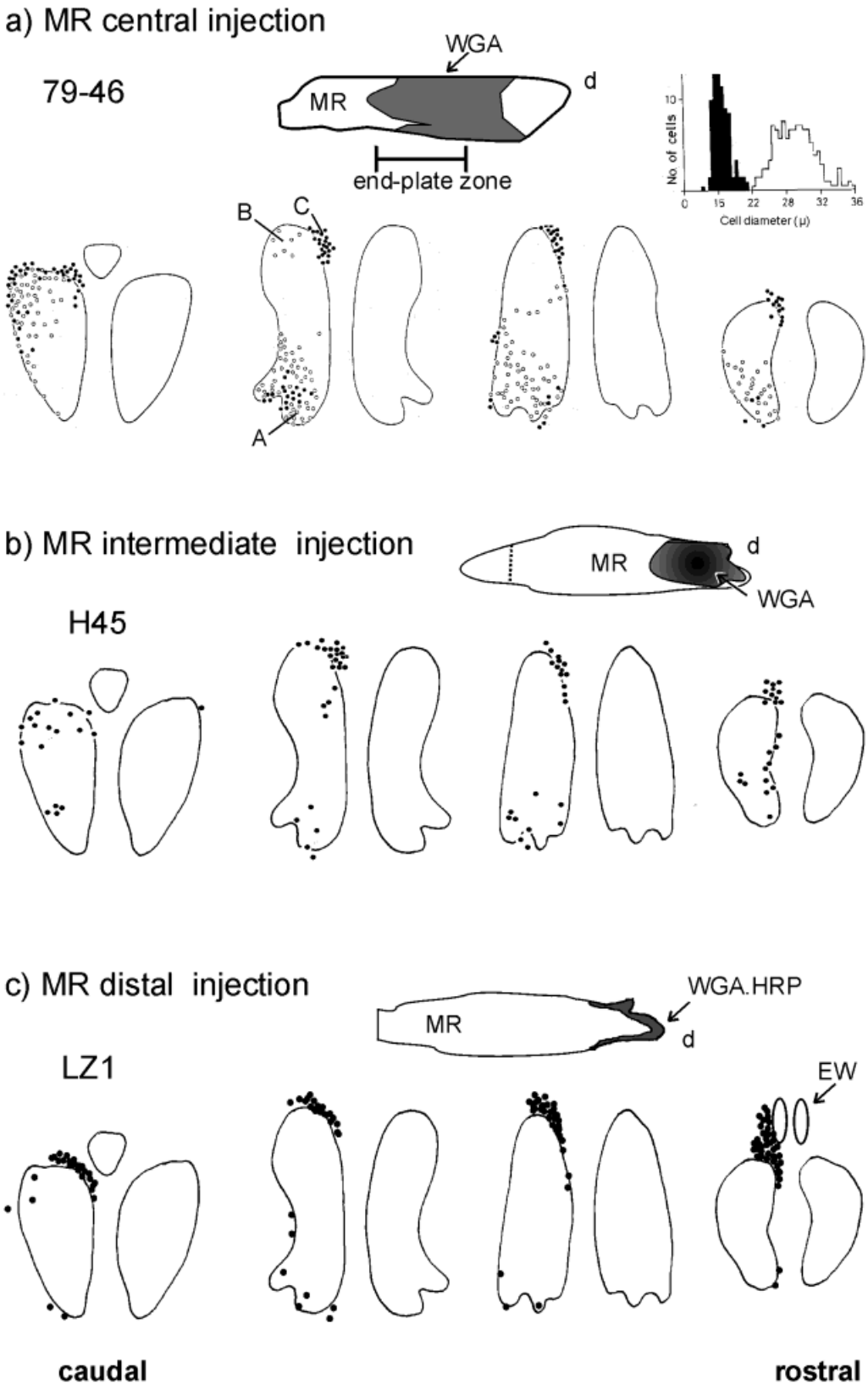

Fig. 7. **a:** The location of large (open circles) and small (black dots) labeled motoneurons in nIII, plotted from single sections at four different rostrocaudal levels, after a central injection of ^{125}I-wheat germ agglutinin (WGA) into the MR muscle. The histogram of their diameters is bimodal, and is divided by eye into small cells (black) and a large cells (open). The tracer-uptake area in MR (shaded area) fills the *en plaque* endplate zone, estimated from synaptophysin-stained sections from a standard case. **b:** The location of labeled motoneurons (black dots) in nIII, plotted from four consecutive sections, at four different rostrocaudal levels, after an injection of ^{125}I-WGA into the distal MR muscle. Compared with a, fewer motoneurons are labeled centrally and more peripherally. **c:** A similar representation of an injection (shaded area) into the myotendinous junction of MR. The retrogradely labeled neurons, taken from two adjacent 40-μm sections, lie almost exclusively around the periphery of the nIII. The peripheral subgroups appear similar to those in a and b at caudal levels, but rostrally, the C-group extends more dorsally toward EW. For abbreviations, see list.

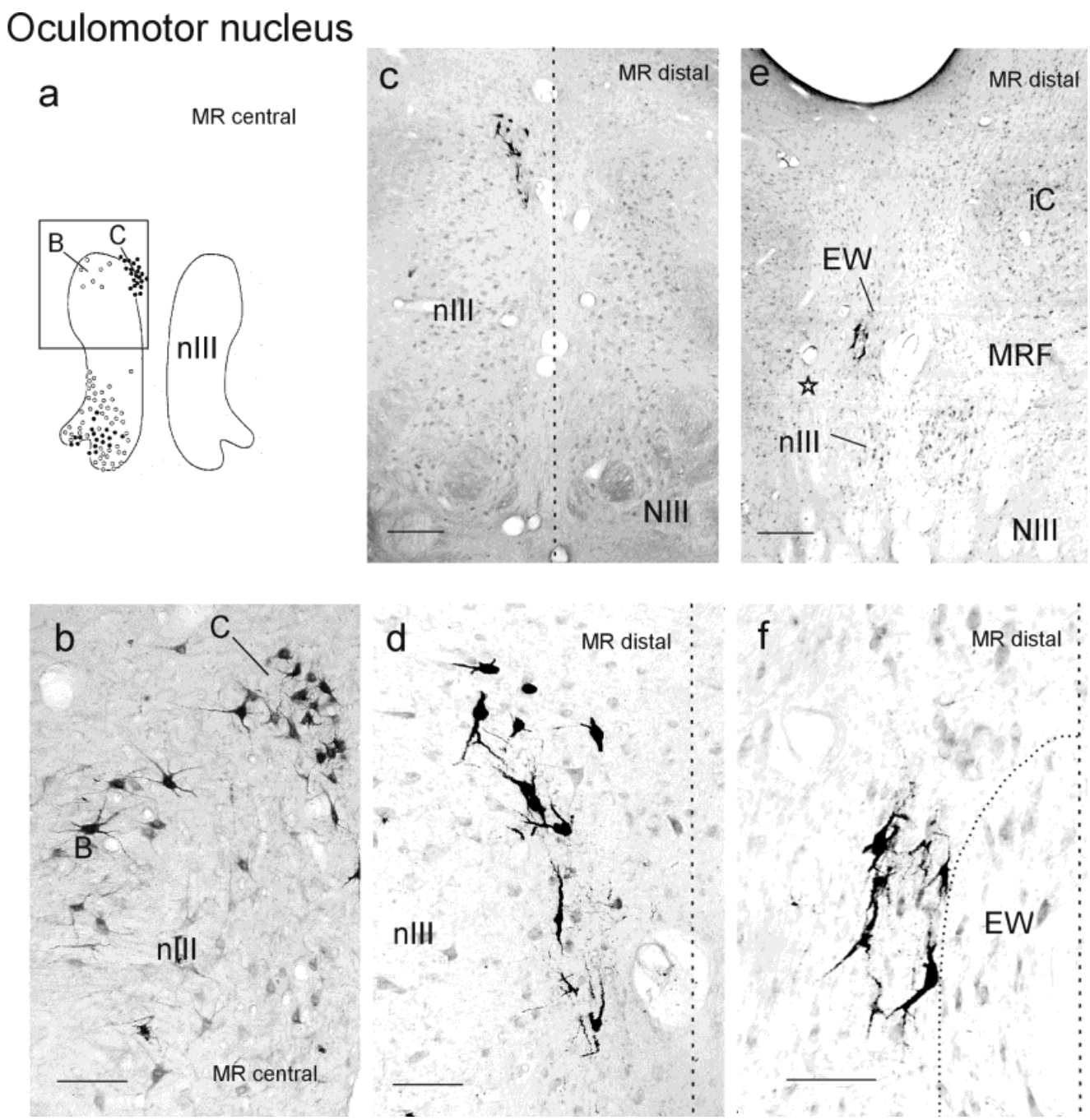

Fig. 8. The charting and photomicrographs in the upper row show retrogradely labeled MR motoneurons (a,c,e), each with an enlargement below in the lower row (b,d,f). **a:** The location of A-, B-, and C-groups in mid-nIII labeled by a multiple injections of wheat germ agglutinin horseradish peroxidase complex (WGA:HRP) tracer into MR (A14-87); the square indicates the region enlarged in (b). **b:** Note, many C-group neurons are smaller in diameter than those in the B-group. **c:** Note the intense labeling of the C-group after a *distal* injection into MR (case LZ1). The weak labeling of the A- and B-groups is not visible. **d:** The C-group neurons shown in c at a higher magnification. Note the presence of several large labeled neurons. **e:** The rostral-most neurons of the C-group labeled by a *distal* injection into MR, which lie immediately adjacent to EW. The asterisk marks one of the regions containing labeled dendritic ramifications in supraoculomotor area. For abbreviations, see list. Scale bars = 300 μm in c,e, 100 μm in b,d,f.

SO), always weakly labeled some large neurons in the classic groups (not shown here). The weak labeling could either be the result of some tracer-spread into SIF endplate areas, uptake by impaled nerves, or due to modest uptake by the *en grappe* terminals on the distal MIFs. Therefore, it remains unclear whether or not some of the large neurons in the classic subgroups also innervate MIFs.

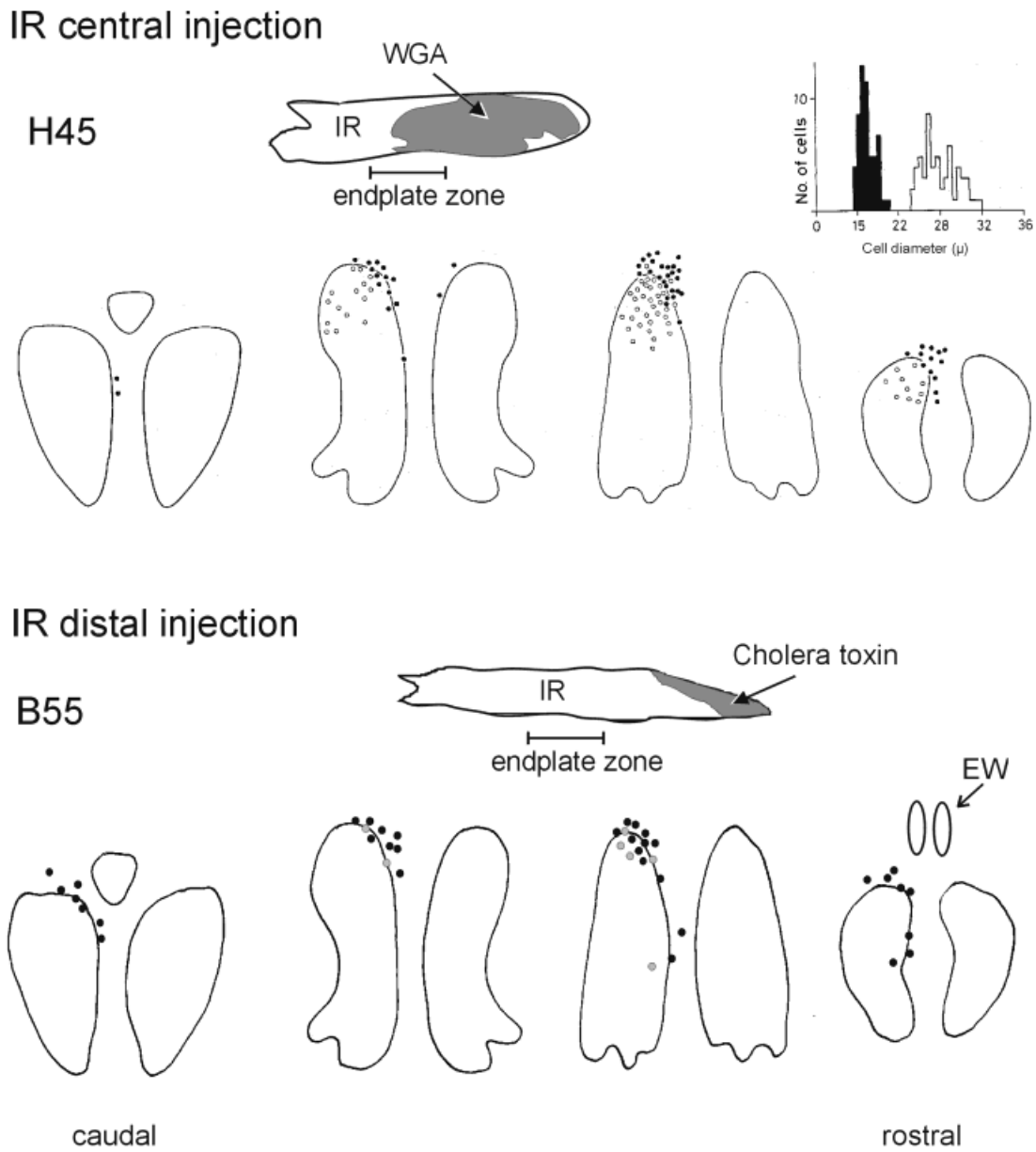

Fig. 9. Upper half: The location of large (open circles) and small (black dots) labeled motoneurons in nIII, plotted from single sections at four different rostrocaudal levels, after a central injection of ^{125}I-wheat germ agglutinin (WGA) into the IR muscle. The histogram of their diameters is bimodal and is divided by eye into small cells (black) and a large cells (open). The tracer-uptake area in IR (shaded area) fills the *en plaque* endplate zone, estimated from synaptophysin-stained sections of an IR muscle, from a standard case. Lower half: A similar representation of a CT injection into the myotendinous junction of IR. The distal uptake area is shaded. Retrogradely labeled motoneurons lie mainly around the periphery of the nucleus, similar to the population of small motoneurons labeled by a central injection. For abbreviations, see list.

Are palisade endings sensory or motor?

Palisade endings are, at present, generally considered to be sensory structures (Alvarado-Mallart RM and Pincon-Raymond M, 1979; Billig et al., 1997; Ruskell, 1999), and it is hard to imagine a motor role for them. However, Lukas et al. (2000) have re-examined palisade endings in humans and decided that some aspects are *motor* in character (e.g., branches with bungarotoxin-binding endplates terminating on distal MIF), whereas other aspects seem sensory. Other lines of evidence also support a motor role for palisade endings, although somewhat indirectly. For example, palisade endings were caused to degenerate by intracranial severance of NIII, NIV, or NVI in monkey (Tozer and Sherrrington, 1910), and again by stereotaxic lesions of the oculomotor nuclei in cat (Sas and Scháb, 1952). Furthermore, Gentle and Ruskell (1997) found too few cell bodies in the sensory trigeminal ganglion of monkey to supply the necessary

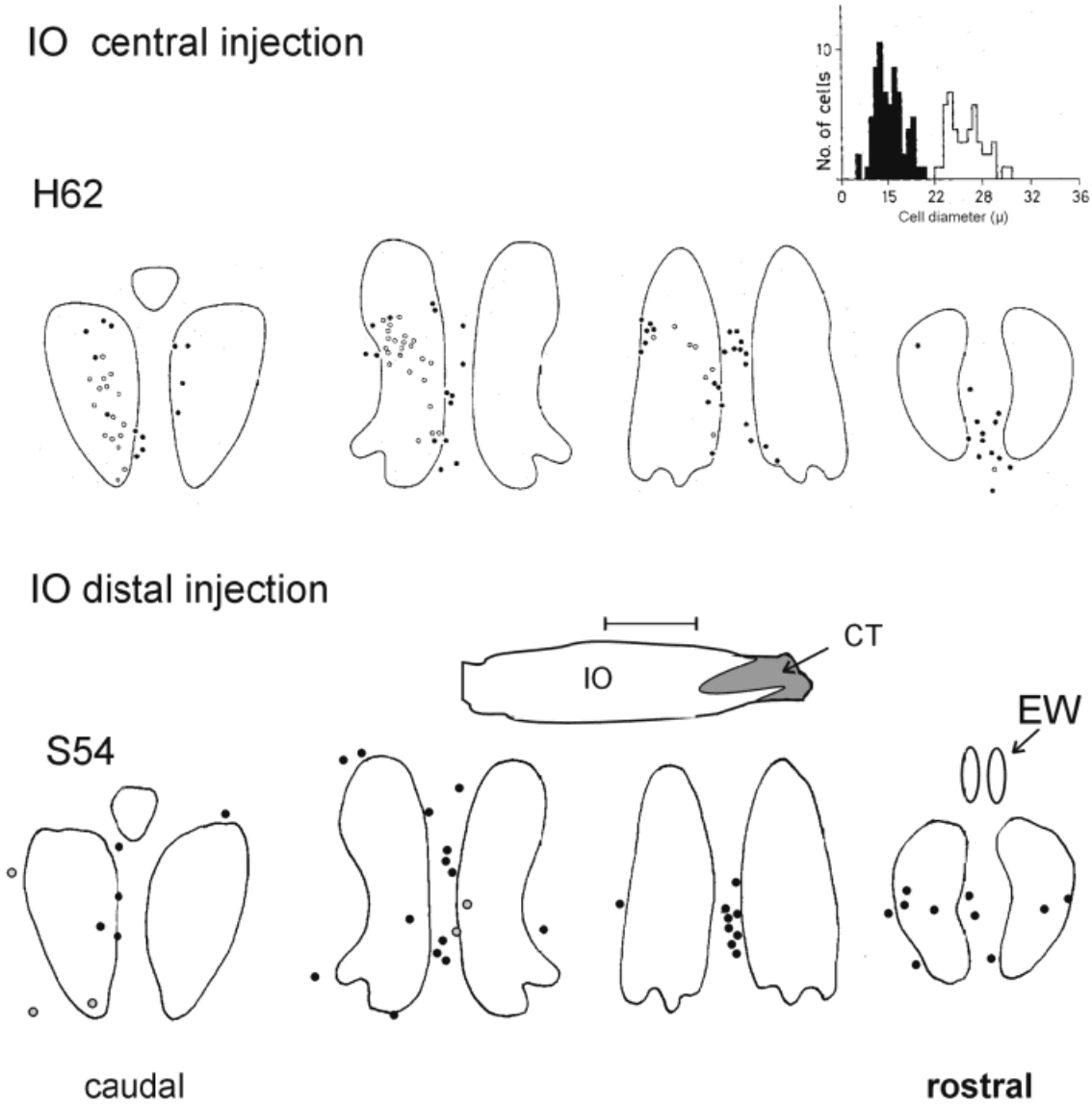

Fig. 10. Upper half: The location of large (open circles) and small (black dots) labeled motoneurons in nIII, plotted from single sections at four different rostrocaudal levels, after a central injection (shaded area) of ^{125}I-wheat germ agglutinin (WGA) into the IO muscle. The histogram of their diameters is bimodal, and is divided by eye into small cells (black) and large cells (open). Lower half: A similar representation of a CT injection into the myotendinous junction of IO. The distal uptake area is shaded and avoids the *en plaque* endplate zone, estimated from synaptophysin-stained sections from this case. Retrogradely labeled motoneurons lie around the periphery of the nucleus, especially bilaterally about the midline.

number of myelinated axons to innervate the palisade endings. We did not systematically investigate the labeling in the trigeminal ganglion in this study; but in the few cases of myotendinous junction injections that we did examine, a few trigeminal ganglion cells were retrogradely labeled.

Our study cannot resolve the question of whether palisade endings are sensory or motor. The cells that were intensely labeled by our injections directly into the palisade terminal region (see Figs. 4, 7, 8) lie immediately adjacent to the motor nuclei, they receive afferents similar to those of motoneurons and have the morphologic characteristics of γ-motoneurons (May et al., 2000) not sensory ganglion cells. However, if it is argued that these cells innervate only the MIF endplates and not the palisade endings, then it is unclear why they are so intensely labeled from the myotendinous junction, unless the MIF motor nerves enter the muscle via the myotenolinous junction.

Separation of large and small motoneurons

According to these experiments, it is a general feature of all the three oculomotor nuclei that smaller motoneurons are not intermingled with the large motoneurons. The anatomic separation of the motoneuron subgroups has important functional consequences. Each subset of mo-

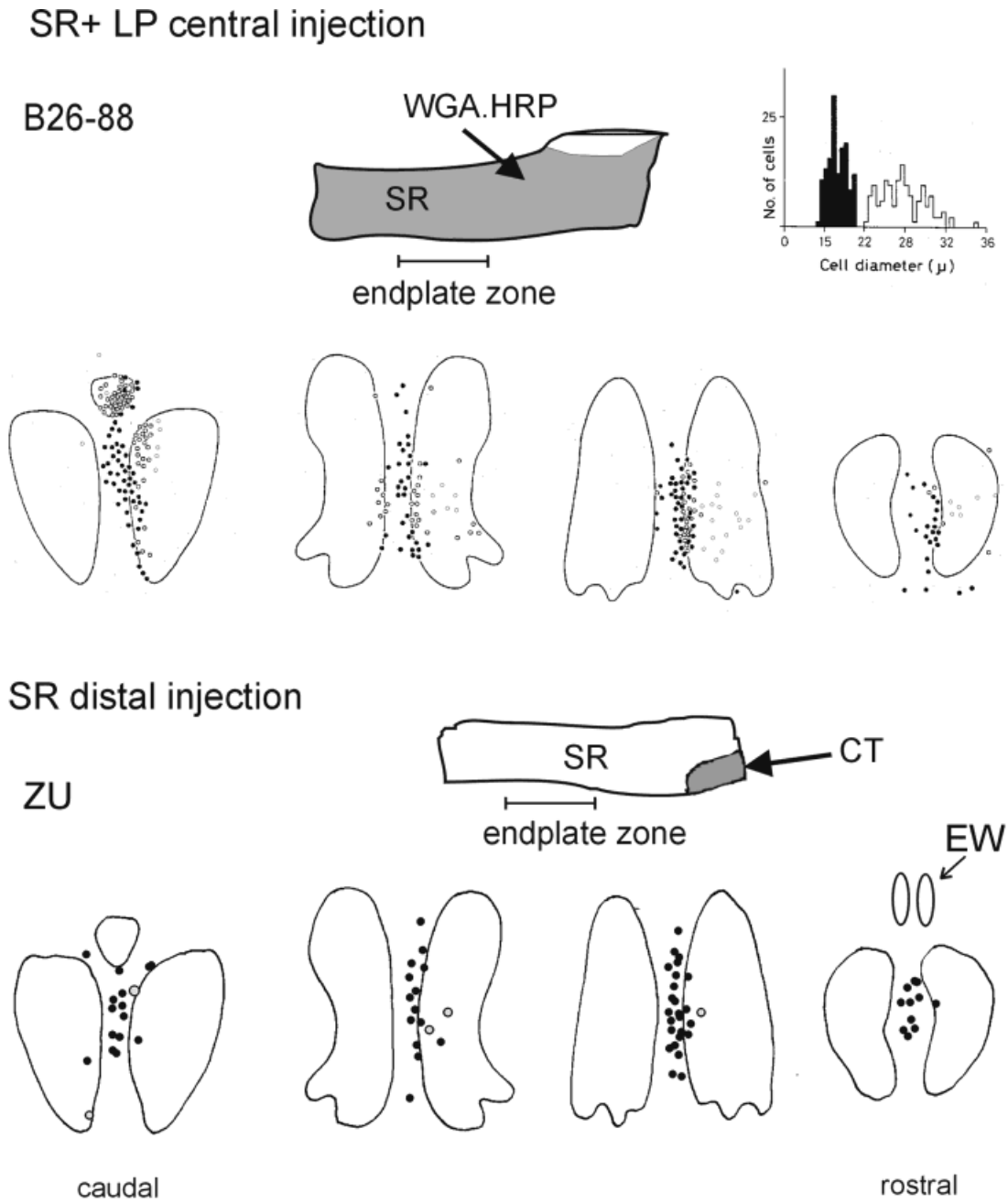

Fig. 11. Upper half: The location of large (open circles) and small (black dots) labeled motoneurons in nIII, plotted from single sections at four different rostrocaudal levels, after a large injection of ^{125}I-wheat germ agglutinin (WGA) into the SR muscle, which also filled the levator palpebrae (LP). The histogram of their diameters is bimodal and is divided by eye into small cells (black) and a large cells (open). The tracer-uptake area in SR (shaded area) fills the *en plaque* endplate zone, estimated from synaptophysin-stained SR sections from a standard case. Lower half: A similar representation of a CT injection into the myotendinous junction of SR. The distal uptake area is shaded. Retrogradely labeled motoneurons lie outside the classic nIII subgroups on the midline bilaterally (like IO), a similar population to the small motoneurons labeled by a central SR injection. For abbreviations, see list.

toneurons could be driven by different afferent pathways. Indeed this is known to be the case: injections of anterograde tracers into the pretectum lead to terminal labeling over the peripheral borders of nIII, including the C-group and midline cell groups, but no terminal labeling over the classic larger motoneuron population of nIII (Büttner-Ennever et al., 1996; Fig. 2b); moreover, only the dorsal cap of the contralateral trochlear nucleus is targeted by efferents of the superior vestibular nucleus, possibly carrying otolith signals (Carpenter and Cowie, 1985). Other afferent pathways to the oculomotor nucleus target both the large and small motoneuron populations (Büttner-

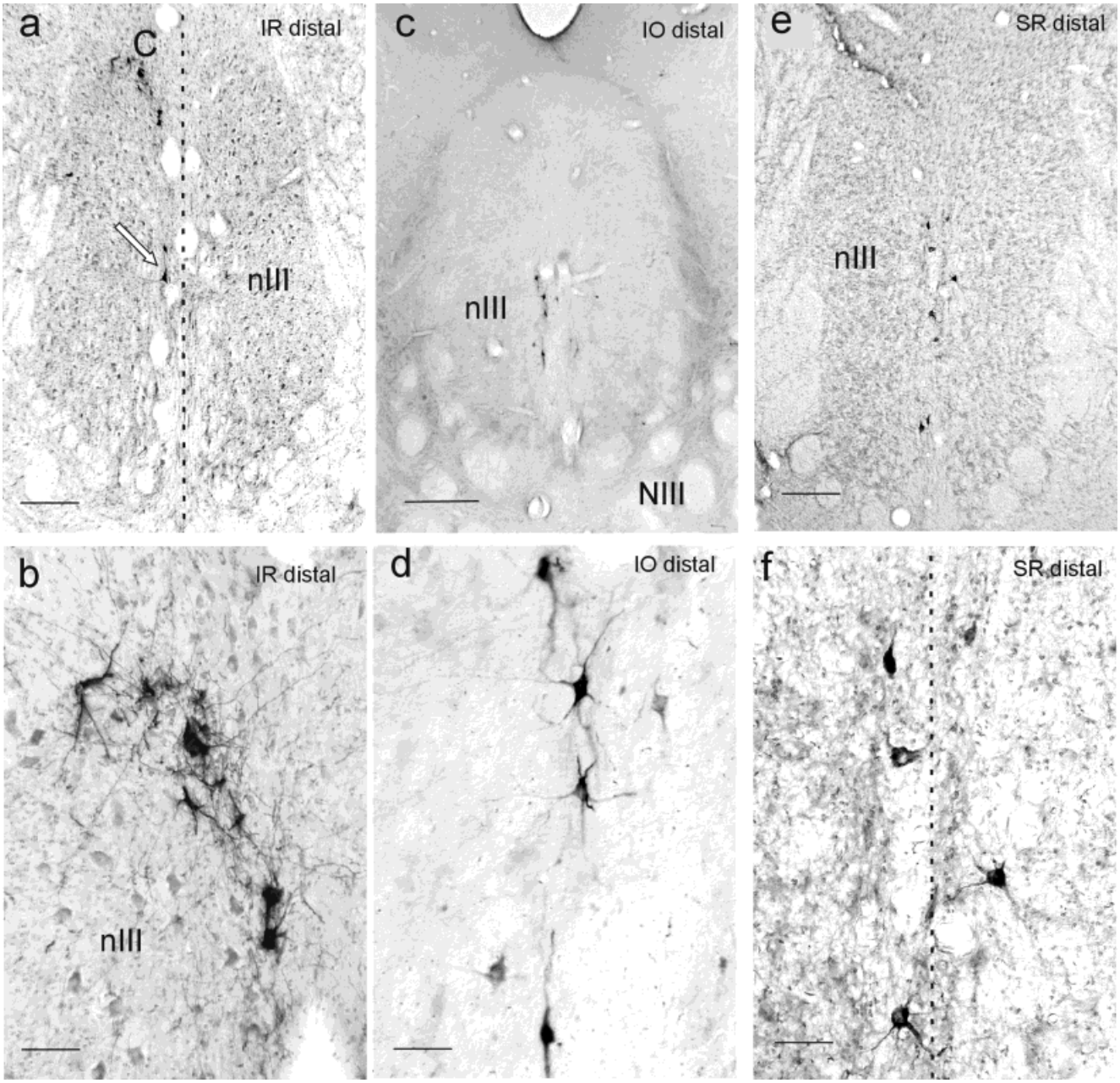

Fig. 12. Upper row: Low-magnification photomicrographs of motoneurons, IR (**a**), IO (**c**), and SR (**e**), retrogradely labeled by injections into the myotendinous junctions of the muscles. **b,d,f:** (Lower row) Enlargements of labeled neurons shown in the upper row. In a and b, IR motoneurons lie in the C-group, the same area labeled from MR. Note their extensive dendrites. In c and f, intensely labeled neurons are found bilaterally on the midline after injections of either IO or SR. For abbreviations, see list. Scale bars = 300 μm in a,e, 500 μm in c, 100 μm in b,d,f.

Ennever and Akert, 1981). These findings underline the idea that there is a functional difference between the large and small motoneuron population.

Organization of MIF motoneurons

The smaller motoneuron population of nIII has a completely different organization than that of the large motoneurons. In the C-group, MR and IR motoneurons of the same eye are intermingled; an afferent input to this subgroup would lead to an adduction of the ipsilateral eye, with a downward component, and a bilateral activation of the C-group would produce vergence. At the midline, between the nIII, where the bilaterally represented IO and SR "MIF" motoneurons are clustered together, an afferent input onto these neurons would cause coactivation of the upward moving muscles of both eyes and produce upgaze. Close to the motoneurons lie a population of medium-large cells that may innervate the palisade endings of the global

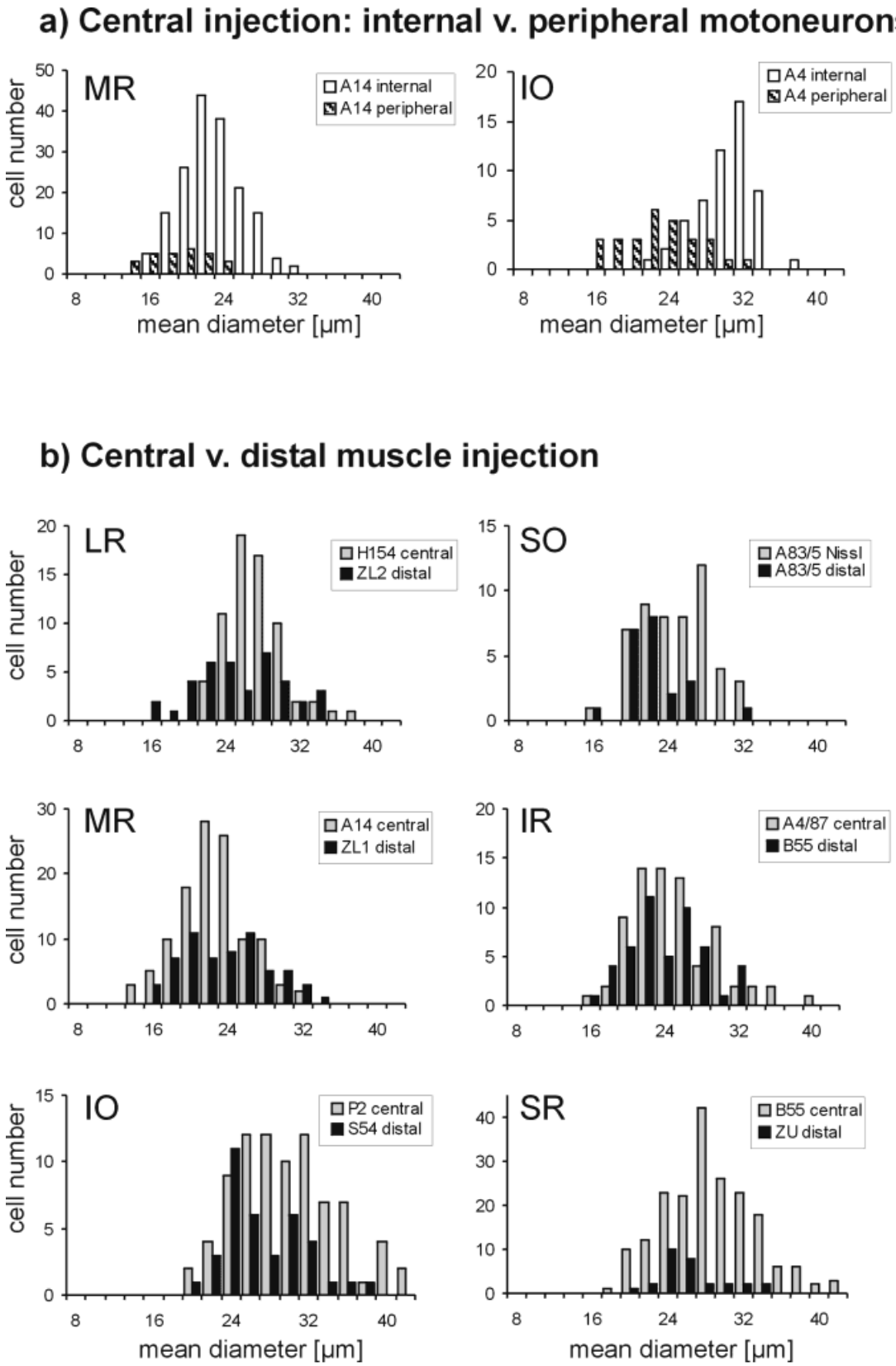

Fig. 13. **a:** Histograms demonstrating the size difference between larger "internal" motoneurons within the motor nuclei and the smaller motoneurons of the peripheral subgroups, labeled after central muscle injections of wheat germ agglutinin:horseradish peroxidase complex (WGA:HRP) into MR and IO. "Internal" MR motoneurons, i.e., subgroups A and B (open bars: $x^{MR} = 22.0$ µm; SD = 2.7; n = 170); peripheral motoneurons, i.e., C-group (striped bars: $x^{MR} = 18.1$ µm; SD = 2.6; n = 27); IO internal motoneurons (open bars: $x^{IO} = 29.3$ µm; SD = 3.1; n = 52); and the peripheral motoneurons (striped bars: $x^{IO} = 21.9$ µm; SD = 4.3; n = 28). **b:** In contrast to a, the populations labeled by central-muscle injections, compared with those labeled by distal-muscle injections, show no significant differences (values given in Tables 1 and 2). This finding suggests that distal injections label an additional population of medium-large neurons within the peripheral subgroups that are not labeled from central muscle injections in a.

TABLE 1. Diameter of Motoneurons Labeled by a *Central* Muscle Injection[1]

Muscle	LR	SO	MR	IR	IO	SR + LP
Case	H154	83-5	A14	A4-87	P2	B55
Tracer	CT	(Neutral red)	WGA:HRP	WGA:HRP	WGA:HRP	WGA:HRP
Mean diameter (μm)	26.4	26.0	21.6	24.1	28.9	27.7
SD	3.2	2.4	3.7	4.7	5.0	4.8
N	67	30	115	72	82	194

[1]See Figure 13b, gray bars. For abbreviations, see list.

TABLE 2. Diameter of Motoneurons Labeled by a *Distal* Injection[1]

Muscle	LR	SO	MR	IR	IO	SR + LP
Case	ZL2	83-5	ZL1	B55	S54	ZU
Tracer	WGA.HRP	WGA.HRP	WGA.HRP	CT	CT	CT
Mean diameter (μm)	24.5	21.3	22.7	23.1	26.0	25.2
SD	4.9	3.1	4.5	3.9	4.3	3.6
N	38	23	61	48	37	29

[1]See figure 13b, striped bars. For abbreviations, see list.

MIFs. These cells would receive a similar afferent input to the MIF motoneurons.

Phylogenetically speaking, oculomotor neuroanatomy is highly conservative, but nevertheless the C-group, innervating MR and IR, has only been described, up until now, in primates (Büttner-Ennever and Akert, 1981; Spencer and Porter, 1981; Sun and May, 1993; McCrea et al., 1986). Ishikawa et al. (1990) unfortunately referred to it as part of the Edinger-Westphal nucleus. Our central and *distal* injections into MR and IR highlighted cells in the C-group, but MR injections also labeled an extension toward EW not seen with central MR muscle injections. The C-group *extension* neurons were found to have very widely spreading dendrites. Those of MR, but not IR, invading EW and the supraoculomotor area. The results confirm those of May et al. (2000), whose EM study revealed synaptic contacts on the ^{MR}C-group dendrites in EW. They considered the ^{MR}C-group neurons to have the structural characteristics of γ-motoneurons. Our results suggest that the C-group may contain several different populations of neurons: MR MIF-motoneurons, IR MIF-motoneurons, and medium-large somata associated with the palisade endings of the global MIFs.

Functional significance of peripheral subgroups

The peripheral subgroups, including the C-group, innervate the MIFs. Robinson (1991) once suggested that the MIFs, with supposedly sensory palisade endings at both ends, resembled an inverted muscle spindle. However, the function of the nontwitch MIFs in extraocular eye muscles is still not known. Several lines of evidence point toward the fact that MIFs do not play a significant role in development of fast muscle forces. First, on stimulation, the nontwitch MIFs produce tonic responses, with weak tetanic tensions. However, they are extremely fatigue resistant and are innervated by slowly conducting axons (Nelson et al., 1986; Dieringer and Precht, 1986). Second, muscle stimulation experiments carried out at the fusion frequency of slow fibers (30/sec) produced no measurable tension changes in the muscle (Fuchs and Luschei, 1971). These features suggest that MIFs and, hence, the peripheral motoneurons, are not suited to contribute significantly to the fast eye movement displacements, but are more suited to playing a role in fixation and stabilizing the eyes around the primary position (Dean, 1996).

The supraoculomotor area and EW are parts of the midbrain near-response region (May et al., 1992). The EW nucleus contains preganglionic neurons driving accommodation of the lens, an essential part of the near-response (Gamlin et al., 1994; May et al., 2000); and recordings made in the supraoculomotor area, dorsal and lateral to nIII, demonstrate neurons carrying premotor vergence signals (Mays, 1984), also an essential component of the near-response and fixation. The close association of the ^{MR}C-group extension with midbrain near-response regions strengthens our previous hypothesis that the C-group may be specialized and play a role in vergence movements (Büttner-Ennever and Akert, 1981).

A reassessment of our hypothesis on the role of the C-group and orbital layer

In our initial experiments on the oculomotor nucleus (Büttner-Ennever and Akert, 1981), we proposed that the small motoneurons of the C-group might innervate the orbital layer. We had placed small tracer injections, aimed at the orbital layer of the MR muscle and retrogradely labeled the C-group, almost exclusively (Büttner-Ennever and Akert, 1981). The injections were mainly in the outer orbital layer, but they were also confined to the distal half of the muscle, and, therefore, targeted predominantly the MIFs. They did not significantly involve the central endplate zone of the orbital layer (Büttner-Ennever and Akert, 1981; see Fig. 3). In addition, orbital MIFs do not have palisade endings. Therefore, in the light of the present experiments, our original conclusion is wrong and should probably be modified to: ". . . small motoneurons in the C-group innervate *the MIFs* of the orbital layer."

In our present experiment, it is impossible to say how much of the orbital layer is involved in the injections. Morphologic studies report that the orbital layer of extraocular eye muscles does not extend as far distally into the tendon as the global layer (Spencer and Porter, 1988), and conversely the global layer MIFs extend furthest into the tendon (Mayr et al., 1975). Therefore, it seems that our present injections into the distal myotendinous junction have primarily targeted the *MIFs of the global layer*, possibly along with their palisade endings, whereas the pre-

vious injections (Büttner-Ennever and Akert, 1981) mainly involved the *MIFs of the orbital layer*. In both sets of experiments, the peripheral neurons of the C-group were labeled, suggesting that both orbital and global layer MIFs are innervated by the peripheral neurons.

The orbital layer MIFs appear to be more complicated than the global MIFs, because they change from a nontwitch MIF character at the fiber extremities to a twitch (SIF) morphology in the central region (Pachter, 1984; Jacoby et al., 1989). Recent reports by Demer et al. (2000) provide several lines of evidence showing that the orbital layer terminates around the capsule of Tenon and controls the tension in the connective tissue "pulleys" surrounding the eye muscles. Taken together, our results suggest that the peripheral motoneurons could control, amongst other things, the tension in the pulleys through the orbital MIFs.

Clinical applications

Two lines of clinical evidence support the role of palisade endings and MIFs in determining eye position (Steinbach, 1987, 2000). One line comes from strabismus patients in which damage to the musculotendinous region, for example in marginal myotomy, was shown to affect the assessment of eye position (Steinbach and Smith, 1981; Steinbach et al., 1987). The second, is the experiments of Dell'Osso et al. (1999), who performed a tenotomy on the eye muscles of dogs with congenital nystagmus, followed by re-insertion at exactly the same position. Surprisingly, the operation led to the reduction of the nystagmus. These results are interpreted by the authors in terms of the MIF-palisade endings being a sensory afferent system, which is damaged by manipulations of the tendon. Even though this interpretation may be in question, their results have far reaching consequences for ophthalmic surgery, emphasizing the need to protect the myotendinous region of the extraocular eye muscles, as do the results of this study.

In conclusion, we have shown that separate groups of motoneurons around the periphery of the motor nuclei, i.e., nIII nIV, and nVI, supply innervation to the nontwitch MIF of the eye muscles. These nerves are thought to innervate the MIFs of both the orbital and the global layers of the eye muscle. However, several questions remain unclear: Do the peripheral subgroups also innervate the palisade endings of the global MIFs? Are the palisade endings sensory or motor structures? Because the peripheral cell groups do not appear to be a homogeneous population, especially in the case of medial rectus, what is the internal organization of the C-group? Further experiments are necessary to answer these questions and to understand the function of MIFs. A whole new set of motoneurons innervating the MIFs have now come to light, and, at present, we have no knowledge of their physiological properties in awake animals. However, because we now know their exact location, experiments investigating their firing patterns, and their premotor inputs are at last feasible. It is not unreasonable to expect that these may well lead to an insight into the illusive problem of the sensory control of eye muscles.

ACKNOWLEDGMENTS

The authors thank Professor W. Lange for his support and Ahmed Messoudi, M.Phil., and Ursula Schneider for their excellent technical support.

LITERATURE CITED

Alvarado-Mallart RM, Pincon-Raymond M. 1979. The palisade endings of cat extraocular muscles: a light and electron microscope study. Tissue Cell 11:567–584.

Augustine JR, Deschamps EG, Ferguson JGJ. 1981. Functional organization of the oculomotor nucleus in the baboon. Am J Anat 161:393–403.

Baker R. 1998. From genes to behavior in the vestibular system. Otolaryngol Head Neck Surg 119:263–275.

Billig I, Buisseret-Delmas C, Buisseret P. 1997. Identification of nerve endings in cat extraocular muscles. Anat Rec 248:566–575.

Bondi AY, Chiarandini DJ. 1983. Morphologic and electrophysiologic verification of multiply innervated fibers in rat extraocular muscles. Invest Ophthalmol Vis Sci 24:516–519.

Büttner-Ennever JA. 2000. A dual motor control of extraocular eye muscles. Neuro-ophthalmol 23:147–149.

Büttner-Ennever JA, Akert K. 1981. Medial rectus subgroups of the oculomotor nucleus and their abducens internuclear input in the monkey. J Comp Neurol 197:17–27.

Büttner-Ennever JA, d'Ascanio P, Gysin R. 1982. The localization of large and small motoneurons in the oculomotor complex of the monkey. In Roucoux A, Crommelinck M, editors. Physiological and pathological aspects of eye movements. The Haugue, Boston, London: Dr W. Junk Publ. p 345–349.

Büttner-Ennever JA, Cohen B, Horn AKE, Reisine H. 1996. Pretectal projections to the oculomotor complex of the monkey and their role in eye movements. J Comp Neurol 366:348–359.

Büttner-Ennever JA, Horn AKE, Scherberger H-J, Henn V. 1998. The localization of motoneurons innervating slow extraocular eye muscle fibers in monkey. Soc Neurosci Abstr 24:145

Carpenter MB, Cowie RJ. 1985. Connections and oculomotor projections of the superior vestibular nucleus and cell group "y." Brain Res 336:265–287.

Dean P. 1996. Motor unit recruitment in a distribution model of extraocular muscle. J Neurophysiol 76:727–742.

Dell'Osso LF, Hertle RW, Williams RW, Jacobs JB. 1999. A new surgery for congenital nystagmus: effects of tenotomy on an achiasmatic canine and the role of extraocular proprioception. J Am Acad Pediatr Ophthalmol Strab 3:166–182.

Demer JL, Oh SY, Poukens V. 2000. Evidence for active control of rectus extraocular muscle pulleys. Invest Ophthalmol Vis Sci 41:1280–1290.

Dieringer N, Precht W. 1986. Functional organization of eye velocity and eye position signals in abducens motoneurons of the frog. J Comp Physiol 158:179–194.

Dogiel AS. 1906. Die Endigungen der sensiblen Nerven in den Augenmuskeln und deren Sehnen beim Menschen und den Säugetieren. Arch Anat Micros Morphol 6:501–526.

Fuchs AF, Luschei ES. 1971. Development of isometric tension in simian extraocular muscle. J Physiol (Lond) 219:155–166.

Gamlin PD, Zhang Y, Clendaniel RA, Mays LE. 1994. Behavior of identified Edinger-Westphal neurons during ocular accommodation. J Neurophysiol 72:2368–2382.

Gentle A, Ruskell GL. 1997. Pathway of the primary afferent nerve fibers serving proprioception in monkey extraocular muscles. Ophthalmic Physiol Opt 17:225–231.

Horn AKE, Hoffmann K-P. 1987. Combined GABA-immunocytochemistry and TMB-HRP histochemistry of pretectal nuclei projecting to the inferior olive in rats, cats and monkeys. Brain Res 409:133–138.

Ishikawa S, Sekiya H, Kondo Y. 1990. The center for controlling the near reflex in the midbrain of the monkey: a double labelling study. Brain Res 519:217–222.

Jacoby J, Chiarandini DJ, Stefani E. 1989. Electrical properties and innervation of fibers in the orbital layer of rat extraocular muscles. J Neurophysiol 61:116–125.

Keller EL. 1973. Accommodative vergence in the alert monkey: motor unit analysis. Vision Res 13:1565–1575.

Keller EL, Robinson DA. 1972. Abducens unit behavior in the monkey during vergence movements. Vision Res 12:369–382.

Lennerstrand G, Baker R. 1987. Motoneural innervation and mechanical properties of extraocular muscles in the catfish, (*Ictalurus punctatus*). Acta Physiol Scand 131:361–369.

Lukas JR, Blumer R, Denk M, Baumgartner I, Neuhuber W, Mayr R. 2000. Innervated myotendinous cylinders in human extraocular muscles. Invest Ophthalmol Vis Sci 41:2422–2431.

Mayr R, Gottschall J, Gruber H, Neuhuber W. 1975. Internal structure of cat extraocular muscle. Anat Embryol (Berl) 148:25–34.

May PJ, Porter JD, Gamlin PD. 1992. Interconnections between the primate cerebellum and midbrain near-response regions. J Comp Neurol 315:98–116.

May PJ, Wright NF, Lin RCS, Erichsen JT. 2000. Light and electron microscopic features of medical rectus C-subgroup motoneurons in macaques suggest near triad specializations (abstract). Invest Ophthalmol Vis Sci 41:4353.

Mays LE. 1984. Neural control of vergence eye movements: convergence and divergence neurons in midbrain. J Neurophysiol 51:1091–1108.

Mays LE, Porter JD. 1984. Neural control of vergence eye movements: activity of abducens and oculomotor neurons. J Neurophysiol 52:743–761.

McClung RJ, Shall MS, Goldberg SJ . 2001. Motoneurons of the lateral rectus and medial rectus extraocular muscles in squirrel monkey and cat. Cells Tissues Organs 168:220–227

McCrea R, Strassman A, Highstein SM. 1986. Morphology and physiology of abducens motoneurons and internuclear neurons intracellularly injected with horseradish peroxidase in alert squirrel monkey. J Comp Neurol 243:291–308.

Mesulam MM. 1978. Tetramethylbenzidine for horseradish peroxidase histochemistry: a non-carcinogenic blue reaction product with superior sensitivity for visualization of neuron afferents and efferents. J Histochem Cytochem 26:106–117.

Morgan DL, Proske U. 1984. Vertebrate slow muscle: its structure, pattern of innervation, and mechanical properties. Physiol Rev 64:103–138.

Nelson JS, Goldberg SJ, McClung JR. 1986. Motoneuron electrophysiological and muscle contractile properties of superior oblique motor units in cat. J Neurophysiol 55:715–726.

Pachter BR. 1984. Rat extraocular muscle. 3. Histochemical variability along the length of multiply-innervated fibers of the orbital surface layer. Histochemistry 80:535–538.

Porter JD, Baker RS. 1998. Anatomy and embryology of the ocular motor system. In: Miller NR, Newman NJ, editors. Clinical neuro-ophthalmology. Baltimore, London, Paris, Munich: Williams & Wilkins. p 1043–1099.

Richmond FJR, Johnston W, Baker RS, Steinbach MJ. 1984. Palisade endings in human extraocular muscle. Invest Ophthalmol Vis Sci 25: 471–476.

Robinson DA. 1970. Oculomotor unit behavior in the monkey. J Neurophysiol 38:393–404.

Robinson DA. 1991. Overview, in vision and vision dysfunction. In: Carpenter RHS, editor. Eye movements. Boca Raton: CRC Press. p 320–331.

Ruskell GL. 1978. The fine structure of innervated myotendinous cylinders in extraocular muscles of rhesus monkey. J Neurocytol 7:693–708.

Ruskell GL. 1999. Extraocular muscle proprioceptors and proprioception. Prog Retinal Eye Res 18:269–291.

Sas J, Schább R. 1952. Die sogennanten “Palisaden-Endigungen” der Augenmuskeln. Acta Morph Acad Sci Hung 2:259–266.

Schnyder H. 1984. The innervation of the monkey accessory lateral rectus muscle. Brain Res 296:139–144.

Scott AB, Collins CC. 1973. Division of labor in human extraocular muscle. Arch Ophthalmol 90:319–322.

Shall MS, Sorg PJ, McClung JR, Gilliam EE, Goldberg SJ. 1995. Relationship of the mechanical properties of the cat inferior oblique muscle to the anatomy of its motoneurons and nerve branches. Acta Anat 153: 151–160.

Siebeck R, Krüger P. 1955. Die histologische Struktur der äußeren Augenmuskeln als Ausdruck der Funktion. Grafes Arch Ophthalmol 156: 637–652.

Spencer RF, Porter JD. 1981. Innervation and structure of extraocular muscles in the monkey in comparison to those of the cat. J Comp Neurol 198:649–665.

Spencer RF, Porter JD. 1988. Structural organization of the extraocular muscles. Rev Oculomot Res 2:33–79.

Steinbach MJ. 1987. Proprioceptive knowledge of eye position. Vision Res 27:1737–1744.

Steinbach, MJ. 2000. The palisade ending: an afferent source for eye position information in humans. In: Lennerstrand G, Ygge J, Laurent T, editors. Advances in strabismus research: basic and clinical aspects. London: Portland Press. p 33–42.

Steinbach M, Smith D. 1981. Spatial localization after strabismus surgery: evidence for inflow. Science 213:1407–1409.

Steinbach MJ, Kirshner EL, Arstikaitis MJ. 1987. Recession vs marginal myotomy surgery for strabismus: effects on spatial localization. Invest Ophthalmol Vis Sci 28:1870–1872.

Sun W, May PJ. 1993. Organization of the extraocular and preganglionic motoneurons supplying the orbit in the Lesser Galago. Anat Rec 237: 89–103.

Tozer FM, Sherrington CS. 1910. Receptors and afferents of the third, fourth and sixth cranial nerve. Proc R Soc Lond 82:450–457.

Warwick R. 1953. Representation of the extraocular muscles in the oculomotor nuclei of the monkey. J Comp Neurol 98:449–495.

Wasicky R, Zhya-Ghazvini F, Blumer R, Lukas JR, Mayr R. 2000. Muscle fiber types of human extraocular muscles: a histochemical and immunohistochemical study. Invest Ophthalmol Vis Sci 41:980–990.